PERGAMON

Vision Research 39 (1999) 3011–3023

Vision Research

www.elsevier.com/locate/visres

Second-site adaptation in the red–green detection pathway: only elicited by low-spatial-frequency test stimuli

C.F. Stromeyer III [a,b,*], P.D. Gowdy [a,b], A. Chaparro [c], R.E. Kronauer [a]

[a] *Division of Engineering and Applied Sciences, Harvard University, Cambridge, MA 02138, USA*
[b] *Department of Psychology, Harvard University, Cambridge, MA 02138, USA*
[c] *Department of Psychology, Witchita State University, Witchita, KS 67260, USA*

Received 25 August 1998; received in revised form 2 December 1998

Abstract

The red–green (RG) detection mechanism was revealed by measuring threshold detection contours in the L and M cone contrast plane for sine-wave test gratings of 0.8–6 c deg^{-1} on bright adapting fields of yellow or red. The slope of the RG detection contours was unity, indicating that the L and M *contrast* signals contribute equally (with opposite signs) on both the yellow and the red fields; this reflects first-site, cone-selective adaptation. Second-site adaptation, which may reflect saturation at a color-opponent site, was evidenced by the RG detection contours being further out from the origin of the cone contrast plane on the red field than on the yellow field. Second-site adaptation was strong (3-fold) for low spatial frequency test gratings but greatly diminished by 6 c deg^{-1}. The disappearance of second-site adaptation with increasing spatial frequency can be explained by spatial frequency channels. The most sensitive detectors may comprise a low spatial frequency channel which is susceptible to masking by the chromatic, spatial DC component of the red field. The 6 c deg^{-1} patterns may be detected by a less sensitive, higher frequency channel which is less affected by the uniform red field. The RG spatial frequency channels likely arise in the cortex, implicating a partially central site for the second-site effect.

Keywords: Red–green mechanism; Second-site adaptation; Spatial frequency

1. Introduction

The red–green (RG) detection mechanism can be revealed by measuring threshold detection contours in the L and M cone contrast plane (L',M'). RG can readily be isolated with coarse spatial test stimuli since RG sensitivity is much higher (Stromeyer, Cole & Kronauer, 1985) than luminance (LUM) sensitivity (Fig. 1). Considerable independence of the RG and LUM mechanisms has been shown in studies on threshold summation (Mullen, Cropper & Losada, 1997), contrast adaptation (Krauskopf, Williams & Heeley, 1982; Bradley, Switkes & De Valois, 1988) and noise masking (Sankeralli & Mullen, 1997; Giulianini & Eskew, 1998).

The RG detection mechanism is closely related to the RG hue mechanism. The RG detection contours correctly predict that the locus for suprathreshold flashes in red–green hue cancellation (Thornton & Pugh, 1983) lies midway between the symmetric red and green contours in Fig. 1 (Chaparro, Stromeyer, Chen & Kronauer, 1995). Flashes arrayed parallel to the red contour are indiscriminable from each other when set to a constant multiple above threshold (but not so intense as to stimulate LUM), and similarly for flashes arrayed parallel to the green contour (Calkins, Thornton & Pugh, 1992). This indicates these flashes may be signaled by a single, bipolar red–green mechanism.

The RG detection contours have a slope of unity in the L',M' plane, demonstrating that the L' and M' contrast signals contribute equally, with opposite sign to the RG mechanism (Stromeyer et al., 1985; Cole, Hine & McIlhagga, 1993). This slope of unity has been obtained on adapting fields of widely different colors, indicating that the L and M cones independently adapt, obeying Weber's Law (Stromeyer et al., 1985; Chaparro et al., 1995).

* Corresponding author. Fax: +1-617-4959837.
E-mail address: charles@stokes.harvard.edu (C.F. Stromeyer III)

0042-6989/99/$ - see front matter
PII: S0042-6989(98)00328-9

We can take into account this first-site cone-selective adaptation by plotting the detection contours in the cone-contrast coordinates (Chaparro et al., 1995). If the cone-selective adaptation is complete (fully obeys Weber's Law) and it alone controls the adapted sensitivity, then the RG detection contours obtained on different colored adapting fields should be identical (i.e. *coincide* in the L',M' plane) except for the effects due to measurement error. However, this is clearly not the case since changing the adapting field from yellow to red causes the RG detection contours to shift outward (Stromeyer et al., 1985) by as much as 4-fold (Chaparro et al., 1995) while maintaining unity slope. A similar desensitization is also seen in the classical color discrimination literature (Nagy, Eskew & Boynton, 1987). The outward shift of the RG detection contour is caused by adaptation at a color-opponent second-site. Adapting fields that deviate in color away from a neutral yellow may polarize or saturate the response of the opponent site.

The second-site adaptation causes an *equal* outward shift of the red contour (Fig. 1) and the green contour (Stromeyer et al., 1985; Chaparro et al., 1995). This demonstrates that the second-site effect does not depend on the chromatic sign of the test flash (red vs. green) or the degree to which the flash stimulates the L or the M cones. This is a signature for a color-opponent adaptation process, occurring at a stage after the L and M signals have been combined. Chromatic adaptation with similar properties has been demonstrated in retinal ganglion cells of macaque (Yeh, Lee & Kremers, 1996).

In the present study we measured the second-site effect in the RG mechanism on yellow versus red adapting fields of equated luminance, using sine-wave test gratings from 0.8 to 6 c deg^{-1}. Full detection contours were measured at each spatial frequency to separate the RG and LUM detection mechanisms. The second-site effect was strong for low spatial frequency test patterns and was greatly diminished at 6 c deg^{-1}. These results will help to specify the locus for the second-site effect.

2. Methods

2.1. Apparatus and retinal alignment of red and green gratings

Vertical sine-wave gratings filled a 3.5° dia field. The gratings were superposed on a 4.2° dia monochromatic background seen in Maxwellian view, rendering the central 3.5° test area metameric to 1600 td and 567 nm (greenish–yellow field) or 625 nm (red field). The gratings, viewed directly (not in Maxwellian view), were generated on red and green CRT monitors (Tektronix 608), which were filtered optically and combined with a dichroic mirror (Stromeyer, Kronauer, Ryu, Chaparro & Eskew, 1995). The two monitors were placed at equal distance from the eye. The entire display was viewed monocularly through a 3 mm artificial pupil and achromatizing lens (Powell, 1981) which corrects for the eye's longitudinal and transverse chromatic aberration. Observers were refracted with a spectacle lens mounted against the achromatizing lens, and the head was stabilized using a hard bite bar on a rigid *xyz* translator.

Small head movements can cause a phase shift between the red and green stripes owing to chromatic parallax. The following procedures were used to align the red and green gratings. At the start of a session we displayed 1 c deg^{-1}, red and green square-wave gratings in spatial antiphase. While on the bite bar the observer made tiny adjustments of the spatial frequency and phase of the red grating so that yellow or dark regions were not visible at the edges of the alternating red and green stripes. The following procedure was then used for the higher spatial frequency gratings. Fine red and green gratings (in spatial antiphase) were set to relatively high contrast; the observer then made a tiny horizontal adjustment of the bite bar to find the point where the pattern was least visible. This assured that the red and green gratings were in retinal antiphase, for being just off this point increased the apparent luminance contrast as the gratings were brought partially into phase.

The data for all observers show that chromatic sensitivity falls rapidly with increasing spatial frequency, whereas luminance sensitivity does not fall, suggesting that RG and LUM were indeed isolated. The finest equiluminant gratings (8 c deg^{-1}) at detection threshold appeared as a small central patch of alternating red and green stripes. Additional methods will demonstrate isolation of the RG mechanism.

2.2. Calibration and the cardinal directions for RG and LUM

The spectral radiance of the red and green lights were calibrated at the eyepiece at 1 nm intervals with a radiometer and monochromator (2 nm HBW). These spectral radiance distributions were weighted by the Smith and Pokorny (1975) cone spectral sensitivities to calculate cone contrast. The gratings are represented as vectors in the L',M' cone-contrast plane. Contrast is specified by vector length in this plane, $VL = (L'^2 + M'^2)^{1/2}$ (Eskew, McLellan & Giulianini, 1999). Contrast sensitivity is specified by the reciprocal of the threshold vector length.

Fig. 1 shows two important stimulus directions especially used for the control experiments. Stimuli in the LUM cardinal direction (45–225°) are equichromatic with the same color as the field; this direction is parallel

to the RG contours and hence does not stimulate RG. Similarly, stimuli in the RG cardinal direction are equiluminant with the field; this direction is parallel to the LUM contours and hence does not stimulate LUM. These stimuli will be called luminance and red–green, respectively. (The optimal vector directions for each mechanism are different from these, being *orthogonal* to the detection contour for that mechanism.)

2.3. Threshold measurements

Observers were color-normal according to the Farnsworth–Munsell 100-Hue test or anomaloscope matches.

The observer first adapted several minutes to the field and thresholds were then measured with a 2AFC procedure. Each trial contained two temporal intervals, separated by 200 ms. The test pattern was presented in one interval chosen randomly and the observer attempted to identify the test interval. The contrast of the grating was ramped on for 380 ms with a raised cosine temporal wave, held constant for 560 ms, then ramped off. Tones signaled the stimulus intervals and provided feedback. The absolute spatial phase of the pattern was randomly set on each trial. A single test stimulus was typically used for each run, which contained two randomly interleaved staircases, estimating threshold at the 71% detection level (Wetherill, 1963). Test contrast was changed in 0.1 log steps with 12-bit digital-to-analog converters (used with a voltage attenuator for very low test contrast). Each threshold estimate is based on the geometric mean of the reversals from four or more staircases.

3. Results

3.1. Detection contours from 0.8 to 6 c deg^{-1}

Full detection contours in the L',M' plane were measured for three observers with sine-wave gratings of 0.8–6 c deg^{-1} on the yellow and red fields. Fig. 2 shows the results for three observers (depicted in different columns), with the spatial frequency increasing in proceeding down the rows.

The RG detection contours were fit with a slope of unity, since the equal contribution of the L' and M' signals to RG has been demonstrated using different spatial test patterns (including tiny spots and medium spatial frequencies) and different colored adapting fields (see Section 4). The slope of unity was confirmed in the present study using a luminance masking paradigm (see below). The slope of the LUM contours, however, was left free to vary. Previous work suggests that the slope of the LUM contour is steep (approximately -3), as measured with a 2°, 200 ms flash on either yellow

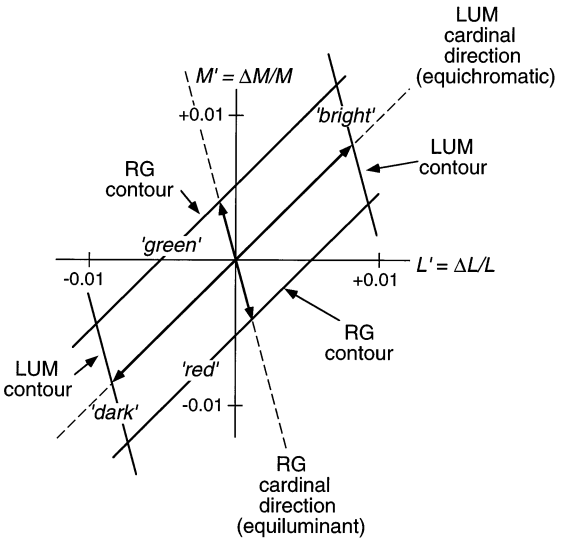

Fig. 1. Hypothetical detection contours for RG and LUM mechanisms in L',M' cone contrast plane. RG has equal and opposite L' and M' cone contrast weights (slope of unity); LUM has L' and M' weights of the same sign, with L dominant (steep negative slope). Contours are defined by thresholds of stimulus vectors like the two shown here representing gratings: in the LUM cardinal direction the vector affects only LUM, while in RG the cardinal direction the vector affects only RG. Along the LUM contours stimuli look *bright* or *dark*; along the RG contours stimuli look *red* or *green*.

(Chaparro et al., 1995) or red fields (Stromeyer, Lee & Eskew, 1992), indicating that the LUM mechanism is dominated by the L' signal. This steep slope was also demonstrated with noise masking (Sankeralli & Mullen, 1997) and the detection of moving LUM gratings (Gegenfurtner & Hawken, 1995; Stromeyer, Chaparro, Tolias & Kronauer, 1997). The present work confirms this steep slope.

At 0.8 c deg^{-1} (Fig. 2, top row) the detection contours on the yellow field are highly elongated along the 45–225° LUM axis, indicating that RG sensitivity is higher than LUM sensitivity. On the red field, the RG and LUM sensitivities are more comparable. For all observers the sensitivity of RG is considerably higher ($\sim$3-fold) on the yellow field than on the red field, demonstrating that there is a large second-site effect at 0.8 c deg^{-1}. The flashes detected by LUM lie on the 45–225° axis; sensitivity to these flashes is fairly similar on the yellow and red fields (as shown latter in Fig. 3, bottom). Shifting from the yellow to the red adapting field produces a considerable decrease in the M cone adapting level (3.4-fold) and slightly increases the L cone level (1.36); however an RG slope of 1.0 fits the RG data well on both fields, indicating good Weberian cone adaptation, consistent with earlier results over a larger adapting range (Chaparro et al., 1995).

At 2 c deg^{-1} (Fig. 2, second row) two differences are seen here relative to 0.8 c deg^{-1}. First, LUM sensitivity has increased considerably at 2 c deg^{-1}—the data

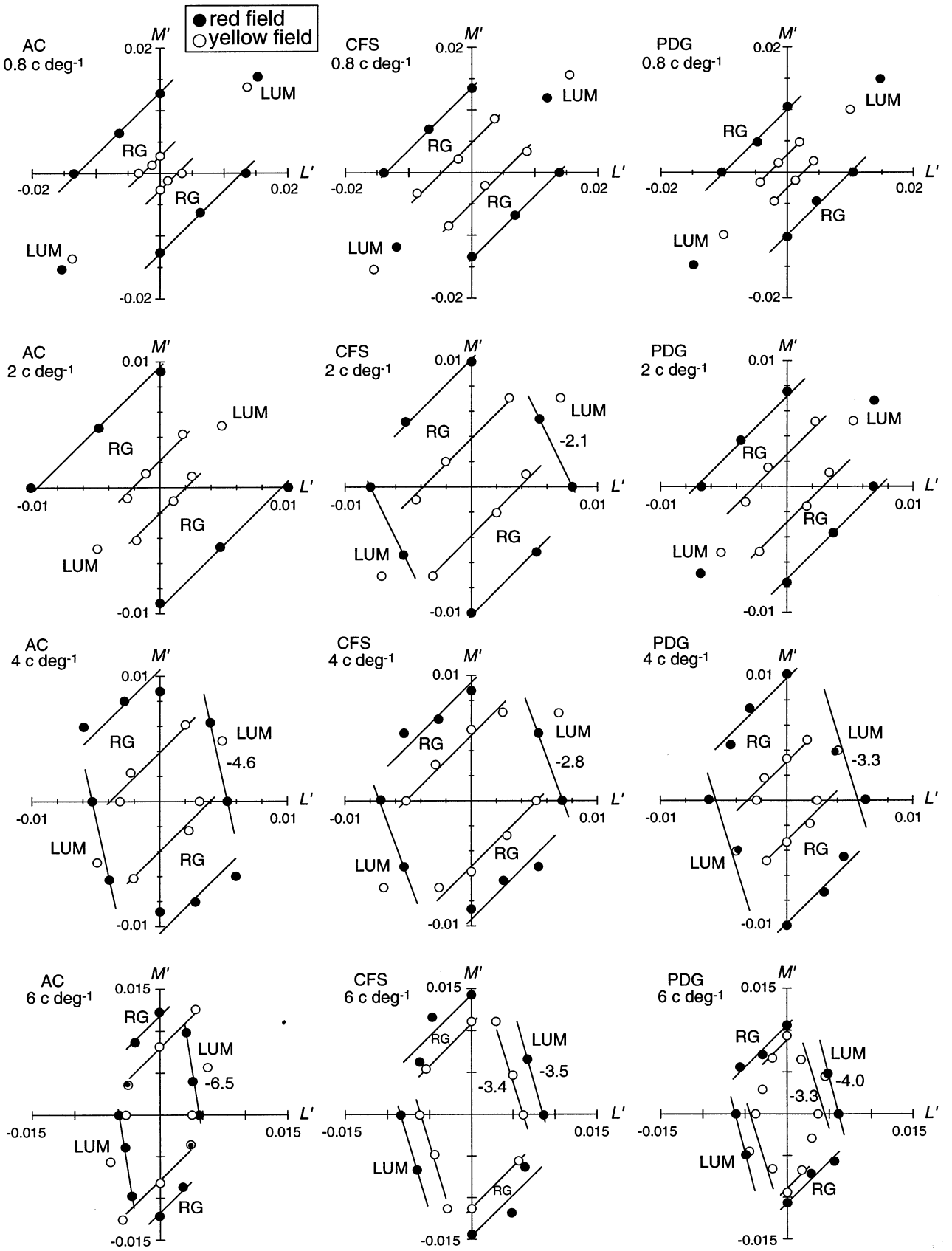

Fig. 2. *Caption opposite.*

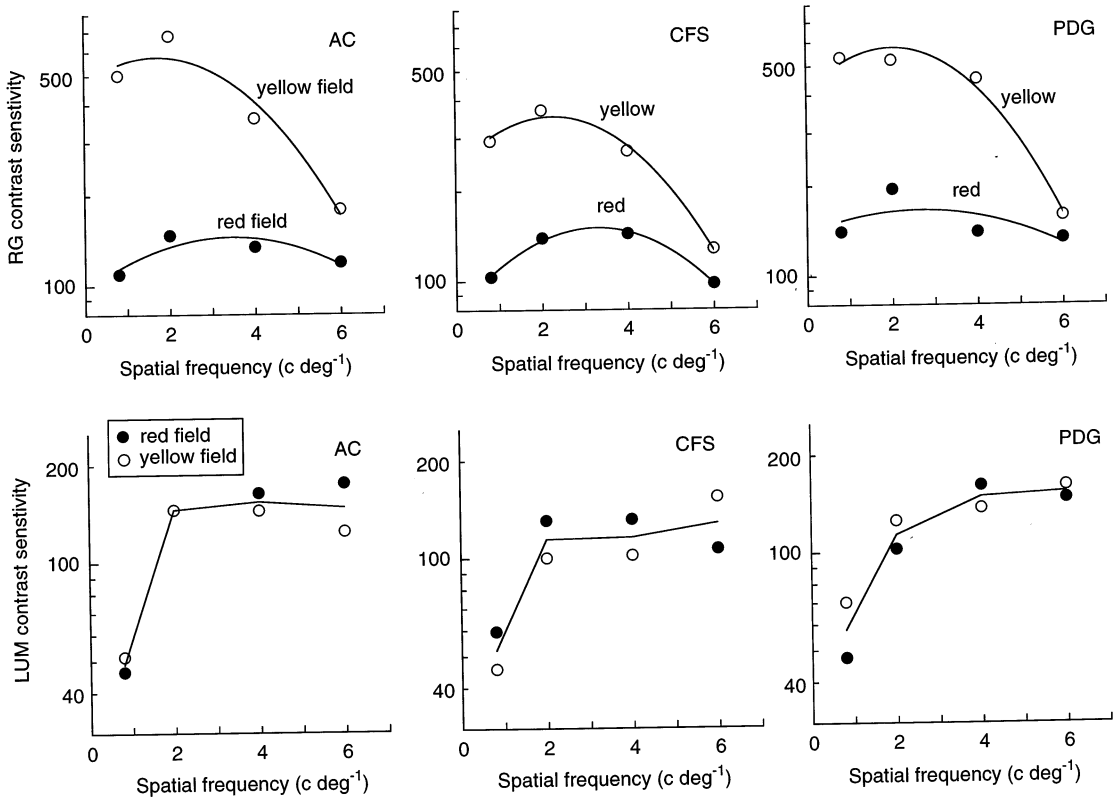

Fig. 3. Top panels: Contrast sensitivity of RG mechanism on yellow and red fields. Sensitivity is based on the 135° vector direction out to the RG contours in Fig. 2. Bottom panels: Contrast sensitivity of LUM mechanism on yellow and red fields. Sensitivity is based on the 45° vector direction out to the LUM contours in Fig. 2. Solid lines depict geometric means for yellow and red fields.

points on the 45–225° axis have moved much closer to the origin (note the axes are magnified 2-fold at 2 vs. 0.8 c deg^{-1} for clarity). This increase of LUM sensitivity is shown more clearly in Fig. 3 (bottom). Second, sensitivity of RG has improved slightly at 2 versus 0.8 c deg^{-1}, especially on the red field (Fig. 3, top). The RG contours fit the data over a considerable extent for the yellow field and over a smaller extent for the red field, owing to the reduced RG sensitivity.

At 4 c deg^{-1} (Fig. 2, third row) the RG contours have moved closer together for the yellow and red fields, and less of the RG contours is revealed because RG sensitivity is declining with increasing spatial frequency while LUM sensitivity remains high (Fig. 3).

Finally at 6 c deg^{-1} (Fig. 2, bottom row), the RG contours have moved even closer together for the yellow and red fields, and even less of the RG contours is revealed. LUM sensitivity remains high at 6 c deg^{-1}, and the LUM contours are steep, showing a strong dominance of the L' signal in LUM. This obscures the extension of the RG contour in the vicinity of the L' axis. Thus, we have fit the RG contours only to data points near the M' axis, lying between the steep LUM contours. (Control experiments will show that the RG mechanism is isolated along the RG contour.) Observers reported that the 6 c deg^{-1} gratings appeared achromatic near the L' axis (hence likely detected by LUM) and chromatic on the M' axis (hence detected by RG). This informal observation will be confirmed with discrimination measurements.

3.2. Contrast sensitivity for RG and LUM

From the detection contours we can derive spatial frequency contrast sensitivity functions for RG and LUM.

The most sensitive (optimal) vector direction for RG is orthogonal to the RG contours, which have a slope of unity. Contrast sensitivity for RG is thus specified by the reciprocal of the vector length in the 135° direction,

Fig. 2. (*Opposite*) Detection contours for sine-wave gratings of 0.8 (top row) to 6 c deg^{-1} (bottom row) on yellow (○) and red (●) fields for three observers (different columns). (Note axes are scaled differently between rows.) Contours for RG are fit with unity slope; the slope of the LUM contours is specified beside the contours. At 0.8 c deg^{-1} sensitivity of RG is 3-times higher on the yellow than red field, and at higher spatial frequencies, the RG detection contours come together on the yellow and red field. Average error ($\pm$1 S.E.M. in % of threshold) at 0.8 c deg^{-1} for AC, CFS, PDG, respectively: 19, 11, 20 (yellow field); 6, 13, 16 (red field); at 2 c deg^{-1}: 15, 7, 16 and 15, 16, 12; at 4 c deg^{-1}: 15, 11, 16 and 12, 8, 5; at 6 c deg^{-1}: 12, 10, 7 and 19, 8,14.

from the origin out to the RG detection contours. (The 315° direction gives the same estimate since the contours are fitted symmetrically.)

Fig. 3 (top) shows the RG contrast sensitivity. On the yellow field, contrast sensitivity is low-pass, falling rapidly with increasing spatial frequency, in agreement with early studies (e.g. Mullen, 1985). The RG sensitivity is very different on the red field, for the sensitivity falls little with spatial frequency and the functions are band-pass, peaking at the middle spatial frequencies. This is remarkable because it demonstrates that the contrast sensitivity function for RG is not invariably low-pass, as is generally assumed.

At low spatial frequency, RG sensitivity is much higher on the yellow field than on the red field, but near 6 c deg^{-1} sensitivity on the two fields is similar. This demonstrates that the second-site effect is confined to low spatial frequencies of the test grating.

Since we do not have good estimates of the slope of the LUM contour at each spatial frequency, we estimate LUM contrast sensitivity simply based on the vector length in the 45° cardinal direction. (The optimal direction will be orthogonal to the LUM contours, but the choice of 45° will yield sensitivity that is approximately a fixed fraction of the true value, independent of spatial frequency.) Sensitivity (Fig. 3, bottom) is similar on the yellow and red fields. Variations in sensitivity between the red and yellow fields may reflect noise since the variations are not consistent between observers. Sensitivity rises sharply from 0.8 to 2 c deg^{-1} and then rises slowly up to 6 c deg^{-1}. The fact that the LUM sensitivity does not fall at 6 c deg^{-1}, whereas RG sensitivity falls considerably, suggests that the RG and LUM mechanisms have indeed been separated.

3.3. Isolating the RG mechanism with a LUM mask

For the above results we fitted the RG contours with a line of unity slope. At higher spatial frequencies, only a small extent of the RG contours was exposed owing to the high LUM sensitivity. We now use a LUM masking paradigm to reveal a larger extent of the RG contours and thus better demonstrate that the slope is unity at each spatial frequency. Regan, Reffin and Mollon (1994) have recently emphasized the usefulness of luminance noise in revealing the chromatic detection mechanisms.

A weak LUM mask grating (a 45–225° vector) was presented in both trial intervals, in spatial quadrature phase (90°) with the test grating and with the same temporal course. The mask contrast was *different for each of the two trial intervals*, randomly chosen from a uniform contrast distribution of about 1.2–3.6-times detection threshold. This contrast randomization (plus the phase quadrature) prevented luminance modulation from serving as an effective detection cue, since the cue is swamped by the large changes in the mask contrast (Gowdy, Stromeyer & Kronauer, 1999). This mask strongly reduced sensitivity of a LUM test on the 45° axis—at 0.8 c deg^{-1} for example, the mask raised threshold 3-fold.

Fig. 4 shows detection contours for RG measured in the presence of the LUM mask on the yellow (top) and red fields (bottom). The data are well fit with contours of unity slope over the full spatial frequency range, 0.8–8 c deg^{-1}. Thus in the presence of the weak LUM mask, the L' and M' signals contribute equally to chromatic detection but with opposite sign.

An undesirable feature is that the LUM mask *facilitates* RG detection by different amounts on the yellow versus red field. Facilitation is defined as the ratio of RG sensitivity with the mask present versus with the mask absent—so a ratio greater than 1.0 indicates facilitation. Fig. 5 shows that the LUM mask clearly facilitates detection of the RG test on the yellow field, but facilitation is considerably weaker on the red field. This agrees with earlier observations which show that an RG spot is clearly facilitated by a coincident LUM pedestal on a yellow field (Cole, Stromeyer & Kronauer, 1990), but the facilitation is considerably weaker on a red field (Chaparro et al., 1995). If the present facilitation had been of equal magnitude at each spatial frequency on the yellow and red fields, then the facilitated thresholds would yield contrast sensitivity functions for the RG mechanism like those in Fig. 3 (obtained without the mask) except for a common vertical scaling factor. The masking results, while not revealing the underlying contrast sensitivity functions for RG, do show that there is an RG mechanism with equal L' and M' inputs at each spatial frequency.

3.4. Control measurements showing that higher spatial frequency gratings are detected by distinct RG and LUM mechanisms on the red field

The results with the weak LUM mask show that there is an RG detection mechanism with equal L' and M' inputs, responsive over the range 0.8–8 c deg^{-1} on the yellow and red fields. However, our spatial contrast sensitivity functions for RG and LUM (Fig. 3) were based on the simple detection thresholds on a *uniform* field employing no mask. At 6 c deg^{-1} rather little of the RG detection contour was revealed owing to the decline of RG sensitivity at this relatively high spatial frequency and the considerable remaining LUM sensitivity. The LUM masking results (Fig. 5) suggest that the small extent of the RG contours seen on the *uniform fields* at the higher spatial frequencies do in fact reflect the presence of the RG mechanism since the LUM mask induces no masking for RG.

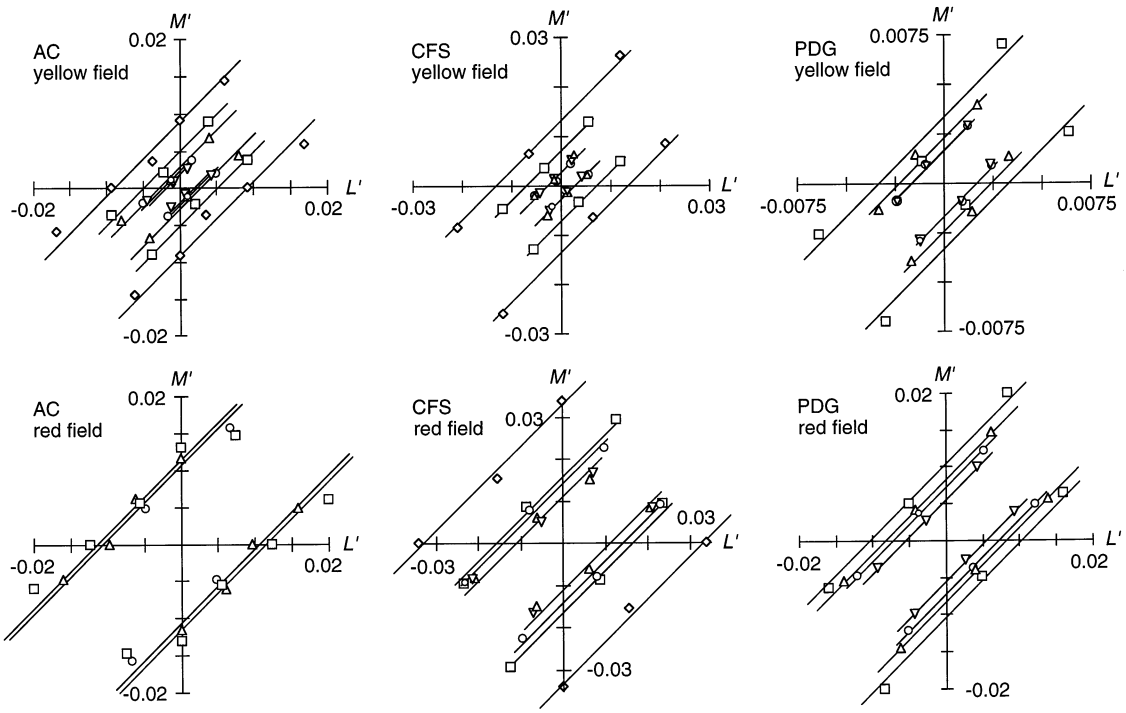

Fig. 4. RG detection contours measured at 0.8–8 c deg^{-1} on yellow and red fields, in presence of LUM mask. Data are well fit by RG contours of unity slope: 0.8 (○), 2(▽), 4 (△), 6 (□) and 8 c deg^{-1} (◇). The scale of the axes varies between panels for clarity.

We have used several additional methods to show that the test gratings in the RG and LUM cardinal directions are in fact detected by the RG and LUM mechanisms, respectively, especially in light of the important argument that detection thresholds alone often do not clearly reveal distinct detection mechanisms (Poirson, Wandell, Varner & Brainard, 1990; Knoblauch & Maloney, 1996). Measurements were made on the red field where we are particularly concerned with showing that the RG mechanism has been isolated. For the present measurements the patterns were of 4 c deg^{-1} so we still have a considerable range of contrast for these control manipulations. Gratings lay in the LUM cardinal direction (45–225°) or the RG equiluminant cardinal direction (100–280°, observer CFS; 107–287°, observer PDG), the latter being roughly estimated from the initial detection contours. These stimuli will be called luminance and red–green.

Three types of measurements with the luminance and red–green gratings demonstrate distinct RG and LUM mechanisms at 4 c deg^{-1} on the red field: (1) detection versus discrimination for static patterns; (2) lack of summation between RG and LUM using a pedestal paradigm; and (3) thresholds for detecting versus identifying the direction of drifting gratings.

3.4.1. (1) Detection versus discrimination of static patterns

If two patterns are detected by separate mechanisms then the two patterns might be discriminated from each other with the same sensitivity as that with which they are detected (Watson & Robson, 1981). Wandell, Sanchez and Quinn (1982) for example showed that on a bright red field, monochromatic red and green flashes of 300 ms duration could be discriminated as well as they were detected. Chaparro et al. (1995) obtained similar results for red and green chromatic flashes on a bright red field.

We randomly intermixed the luminance and red–green gratings within a single run, with two staircases devoted to each of the two patterns. A single pattern was presented on each trial. Detection and discrimination thresholds were measured separately in closely alternating runs.

The ratio of discrimination versus detection *sensitivity* (averaged for the two test patterns) was 1.03 for observer CFS and 0.87 for observer PDG. This indicates that the two patterns are largely detected by separate mechanisms. Observers remarked that the luminance pattern appeared as dark stripes and the red–green pattern appeared as reddish and greenish stripes.

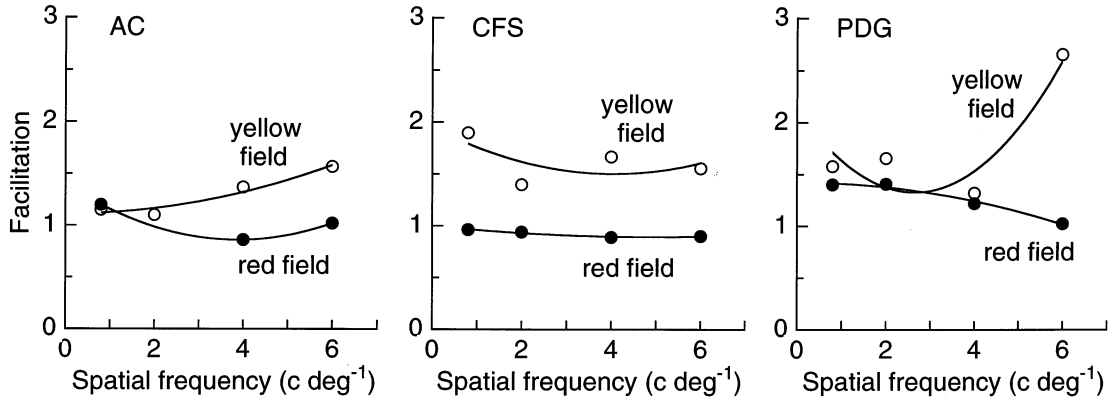

Fig. 5. Facilitation of RG gratings by the LUM mask on the yellow and red fields (Fig. 4). Facilitation is the ratio of sensitivity in the presence of the mask versus in the absence of mask.

The slightly lower discrimination performance for observer PDG might have several causes. First, we are measuring sensitivity at a rigorous level corresponding to $d' = 1.0$; at a slightly higher contrast, discrimination might increase relative to detection. Second, the red field might add a slight field additive redness to the test, possibly causing the dark luminance bars to appear weakly reddish and thus be more confused with the red–green grating. Third, detection of these relatively fine patterns may be partially mediated by orientation information (the patterns typically appeared as vertical stripes at threshold) which might be used more efficiently than simple color information.

3.4.2. (2) Lack of summation between the RG and LUM mechanisms

Mullen et al. (1997) demonstrated a lack of threshold summation between equiluminant red–green and luminance patterns measured up to 4 c deg^{-1} on a yellow field. If summation occurs separately within the RG and LUM mechanisms, then a weak pedestal which stimulates only one of these mechanisms might be used to reveal the detection contour of that mechanism. For example, Chaparro et al. (1995) were better able to reveal the LUM contour for a test spot on the red field using a subthreshold LUM pedestal.

In separate runs, the luminance pedestal grating was set at 1.5-times detection threshold for measuring the LUM contour, and the red–green pedestal was set at 2.0-times detection threshold for measuring the RG contour. The pedestal was presented in both trial intervals, and the test pattern was added spatially in phase with the pedestal in one interval and in antiphase in the other interval. In this phase discrimination task the observer attempts to identify the in phase interval (Stromeyer et al., 1995).

This experiment, although intuitively simple, proved difficult for several reasons. Initially we tried setting the pedestal just slightly suprathreshold, but over the long period required for the measurements sensitivity varied, with the pedestal often falling below threshold. For the final measurements shown here, we set the pedestal more suprathreshold so that it would lie in the flattish region of the dipper function for contrast discrimination. However this gave noisy threshold estimates (requiring many runs), because the psychometric function is typically rather flat for such suprathreshold contrast discrimination.

Fig. 6 shows thresholds for a range of test vectors measured with the luminance (○) and red–green pedestal (●). The detection contours fitted to these data resemble the LUM and RG detection contours originally measured without the pedestal, but the present results isolate the two mechanisms over a larger range of vector orientations, confirming that the RG contour has a slope near unity.

3.4.3. (3) Detection versus identifying the direction of drifting gratings

Metha and Mullen (1998) showed that on a white field the direction of drift (e.g. up vs. down) of luminance gratings of 1.5 c deg^{-1} and 1–16 Hz can be identified at detection threshold, whereas similar red–green equiluminant gratings must be about twice detection threshold for direction identification. We measured similar detection and direction thresholds.

Detection thresholds were measured for the luminance and red–green gratings drifting left versus right. The two types of patterns were used in separate runs, with thresholds simultaneously measured for drift rates of 2 and 4 Hz. For the luminance pattern the ratio of detection sensitivity at 4 versus 2 Hz was 1.02 for observer CFS and 1.17 for PDG, as would be expected for the LUM mechanism (Watson & Turano, 1995). However, for the red–green pattern, detection sensitivity dropped considerably at 4 Hz. The ratio of sensitivity at 4 versus 2 Hz was 0.61 for observer CFS and 0.71 for PDG, consistent with the low-pass temporal fre-

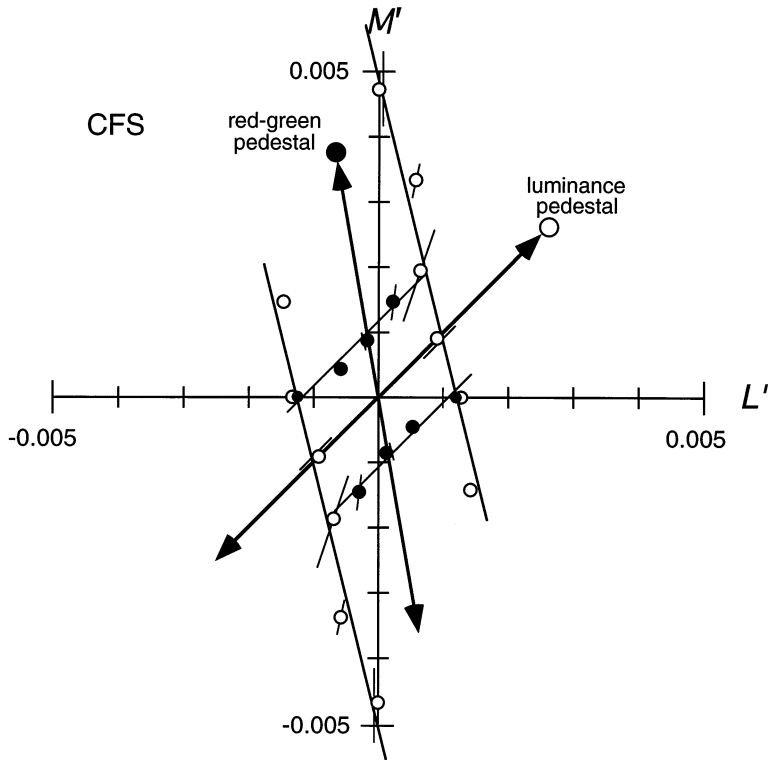

Fig. 6. Detection contours of RG and LUM mechanisms measured on red field at 4 c deg^{-1} in the spatial phase discrimination paradigm. RG contour (●) was assessed with an equiluminant red–green pedestal of 2.0-times detection threshold; LUM contour (○) was assessed with a luminance pedestal of 1.5-times detection threshold. Data points show test thresholds per se. Error bars are ±1 S.E.M.

quency sensitivity for the RG mechanism (Regan & Tyler, 1971).

Direction identification thresholds were measured for the 2 Hz drifting patterns in separate runs (which were intermixed with the detection runs). For the luminance pattern, the direction could be identified at detection threshold—the ratio of identification versus detection sensitivity was 1.03 for observer CFS and 0.96 for PDG. However, for correct direction identification of the red–green pattern the contrast had to be considerably above detection threshold—the ratio of identification versus detection sensitivity was 0.63 for observer CFS and 0.52 for PDG. Observers remarked that the RG pattern also appeared to move much slower than the LUM pattern.

These results show that the drifting 2 and 4 Hz red–green gratings are detected by a chromatic mechanism and not by the luminance mechanism. The *static* red–green pattern used to measure the original detection contours is even more likely to favor detection by the chromatic mechanism, since RG is expected to have low-pass temporal sensitivity.

In summary, these three control measurements show that on the red field the higher spatial frequency, 4 c deg^{-1} luminance and red–green patterns are detected by LUM and RG, respectively, and this would likely be true for the 6 c deg^{-1} gratings as well.

4. Discussion

4.1. Colored adapting fields and the detection of different spatial frequencies: previous findings

Earlier studies showed that low temporal frequency red flicker on a red field (Sternheim, Stromeyer & Khoo, 1979) or low spatial frequency red gratings on a red field (Stromeyer & Sternheim, 1981) actually became *more* visible when green light was added to the adapting field. However, for test stimuli of high temporal or spatial frequency the red and green fields acted approximately additively in elevating threshold. Similarly, Wandell and Pugh (1980b) observed that red and green adapting fields were subadditive in elevating the threshold of a 1° red flash of long duration, 200 ms, but the fields were additive when the flash was brief, 10 ms (Wandell & Pugh, 1980a).

These results do not necessarily reveal the action of the second-site effect when the test is of low temporal or spatial frequency. Red test patterns on the red field are represented by a vector of ~45° in the L',M' plane, so the patterns are likely detected by the LUM mechanism. As uniform green light is added to the adapting field, M cone contrast decreases faster than L cone contrast, causing the test vector (for the red increment) to rotate toward the L' axis. If the detection contour is

elongated in the LUM direction (as will be the case for patterns of low spatial and temporal frequency), then detection may shift from the LUM mechanism to the more *sensitive* RG mechanism (Stromeyer & Sternheim, 1981). There may simply be a shift between detection mechanisms as uniform green light is added to the field. Thus these studies do not establish that there is an adaptable second-site within RG.

Stromeyer and Sternheim (1981) observed that the red and green fields were approximately additive in controlling sensitivity of relatively fine (4 and 12 c deg^{-1}) gratings of monochromatic red light. This result may also not bear on the issue of whether there is a second-site effect in RG at higher spatial frequency because the gratings may have been detected by just the LUM mechanism for *all* the red and green field mixtures. The red gratings on the various fields correspond to test vectors of $\sim$5 to 45° in the L',M' plane (Stromeyer & Sternheim, 1981); the present detection contours suggest that fine gratings of these angles are largely detected by the LUM mechanism on both the red field and the yellow (red-plus-green) field. To clearly reveal a second-site effect in RG it is necessary to isolate RG and LUM by measuring complete detection contours.

4.2. Present results on the second-site effect

The present experiments have attempted to isolate RG and LUM in this manner. The second-site effect in RG was large at low spatial frequency and was greatly diminished at 6 c deg^{-1}.

Although RG sensitivity was strongly suppressed by the second-site effect at low spatial frequencies on the red field, LUM sensitivity (in the 45° vector direction) was fairly similar on the yellow and red fields for spatial frequencies of 0.8–6 c deg^{-1} (Fig. 3, bottom). However, for detecting flicker and motion, the color of the adapting field can strongly affect the relative L' and M' weights in the LUM mechanism, and these relative weights may also change strongly with both temporal and spatial frequency, reflecting an adaptive modification in the receptive field properties of the retinal MC cells (Stromeyer et al., 1997).

4.3. Balanced L′ and M′ inputs to RG and slope of unity

Control measurements showed that the RG mechanism was isolated at higher spatial frequencies on the red field, so that the observed reduction in the second-site effect in RG at higher spatial frequencies cannot simply be ascribed to a shift in detection from the RG to the LUM mechanism. Only a small portion of the RG detection contour was apparent at 6 c deg^{-1} for two reasons: first, LUM sensitivity was slightly higher than RG sensitivity at 6 c deg^{-1}, thus obscuring part of the RG contour, and second, the LUM mechanism is dominated by the L' signal which further obscures the RG contour in the vicinity of the L'-axis.

We nevertheless continued to fit the limited extent of the RG data with a slope of unity for the following reasons. First, measurements with foveal 1 and 2° test spots indicate that the RG contour has a slope of unity on adapting fields ranging from green to deep-red (Stromeyer et al., 1985; Chaparro et al., 1995). Second, Cole, Hine and McIlhagga (1994) obtained a slope of $\sim$1.0 for RG using a 6 c deg^{-1}, foveal circular Gabor pattern on a white field—a target for which RG was at least twice as sensitive as LUM. Third, with our weak LUM mask LUM sensitivity was sufficiently decreased so that chromatic data could be well fit by a slope of unity from 0.8 to 8 c deg^{-1} on the yellow and red fields. Fourth, our three control measurements with the 4 c deg^{-1} gratings on the red field demonstrated that gratings in the LUM and RG cardinal directions stimulated LUM and RG, respectively.

The slope of the RG contour has also been shown to be unity for foveal spots as small as 2.3 min arc on a yellow field (Chaparro, Stromeyer, Kronauer & Eskew, 1994), and detection of these small RG spots was not masked by a relatively intense, coincident LUM pedestal having a vector angle of 45°. The lack of masking is consistent with the view that RG has balanced opponent L' and M' inputs.

Physiological studies show that the red–green PC cells in the retina (Lee, Martin & Valberg, 1989) and LGN (Derrington, Krauskopf & Lennie, 1984) have approximately balanced, opponent L' and M' weights for low spatial frequency stimuli. For higher spatial frequency red–green gratings ($\geq$4 c deg^{-1}), the receptive field center response dominates the surround causing an imbalance of the L' and M' weights (Derrington et al., 1984). The psychophysical threshold for RG shows much higher sensitivity than that of individual PC cells, so the threshold may depend on a central mechanism which gains sensitivity by summing many PC inputs (Chaparro, Stromeyer, Huang, Kronauer & Eskew, 1993). The RG detection mechanism could have balanced L' and M' inputs for foveal spots as small as 2.3 min arc even though the individual PC cell inputs are not fully balanced. For example, the higher mechanism might receive inputs from both + L center and − M center PC cells. Also, a small spot of 2.3 min in central fovea likely does not isolate the center response of a midget red–green PC cell with its single cone input, since the spot is expected to stimulate a random array (Gowdy & Cicerone, 1998) of about 12 L cones and 6 M cones (Cicerone & Nerger, 1989). The slope of unity for the RG detection mechanism for spots as small as 2.3 min suggests that RG has a fixed spectral tuning, in contrast to the hypothesis of a variable-tuned detection mechanism proposed by Finkelstein and Hood (1984)—as discussed in Chaparro et al. (1994).

In summary, RG appears to have a detection contour of unity slope, showing balanced L' and M' inputs over a considerable range of spot sizes and spatial frequencies on both the yellow and red adapting fields.

4.4. Possible mechanisms for spatial-frequency dependence of the second-site effect

Chaparro et al. (1995) summarized possible mechanisms for the second-site effect. The effect may originate in the cone response to the *steady* red field. The photoreceptors become increasingly hyperpolarized as the illumination of a steady field is raised (Kleinschmidt & Dowling, 1975; Normann & Perlman, 1979). Thus the red field may hyperpolarize the L cones more than the M cones, which is not incompatible with first-site, Weberian adaptation occurring independently in the L and M cones—the adaptation may reflect a gain change (Chaparro et al., 1995). Thus, the cones may adapt in a Weberian manner, yet a residual DC signal may remain indicating the level to which the cones are hyperpolarized by the steady field.

The signal reflecting the differential hyperpolarization of the L and M cones must then penetrate deeper into the visual system to create the second-site effect. For example, a *steady* signal could drive the bipolar cells into saturation, as shown by the strong threshold elevation (Hayhoe, 1979) observed for a test spot centered on the afterimage of a small bleaching field; the threshold elevation persists after the afterimage fades from view. The second-site effect may occur partially at the level of the retinal ganglion cells, since Yeh et al. (1996) showed that changes in field color produced strong, long-lasting changes in the cell response.

If such early sites exist then there might be little interocular transfer of the second-site effect. Mollon and Polden (1977) found that a second-site effect in the S cone pathway (transient tritanopia) could not be elicited interocularly. Stromeyer et al. (1997) similarly observed that the large chromatic adaptation effects in the magnocellular-based LUM pathway could not be elicited dichoptically. Earlier, Stromeyer and Sternheim (1981) showed that the increase in sensitivity for a red flash on a red field induced by adding uniform green light to the field was absent when the red stimuli were presented to one eye and the green to the other eye, but it must be noted that the red flash is likely detected by LUM in the dichoptic condition. To reveal a possible interocular second-site effect for RG, further measurements are needed with RG properly isolated.

Although the second-site effect may arise at an early site like the bipolar or ganglion cells, the cortex may also play a role. Adaptation to steady fields may produce a signal that penetrates yet deeper into the visual system, perhaps to the cortex. For example, De Valois and Walraven (1967) observed that an afterimage of a bright red field in one eye strongly changed the hue of a green field in the other eye, even after the afterimage completely faded.

To explain why the second-site effect is strong only at low spatial frequencies, we may consider the idea of a range of spatial frequency channels in the RG pathway. Bradley et al. (1988) have shown that there is little cross spatial adaptation between RG and LUM, and within RG the spatial adaptation is selective for spatial frequency and orientation (with tuning somewhat broader than in LUM). Thus there may exist a range of spatial channels in the RG pathway. This is further supported by measurements showing good discrimination of different spatial frequencies or orientations of RG gratings at detection threshold (Webster, De Valois & Switkes, 1990). The orientation selectivity indicates that these channels are cortical to some extent, and a cortical locus is also supported by the fact that spatial adaptation in RG transfers interocularly to some degree (Chan, De Valois & Switkes, 1986).

The most sensitive RG channel may very well be a low spatial frequency channel comprising big blob detectors (Gowdy et al., 1999). This would account for the high sensitivity with large test spots or low spatial frequency gratings on the yellow field. However these blob detectors might be quite sensitive to the spatial DC chromatic component of the red field, explaining the strongly reduced sensitivity on the red field for tests consisting of large spots or low-frequency grating. The 6 c deg^{-1} RG patterns however might be detected by a different, higher spatial frequency channel, which by being band-pass would be less responsive to the low spatial frequency DC component of the red adapting field. Yang, Qi and Makous (1995) have proposed a similar model in the luminance domain, with the lowest spatial frequency channels being susceptible to masking by the DC component of the luminance field.

Acknowledgements

We thank R.T. Eskew Jr. for comments. Research was supported by NIH EY11246 and A. Chaparro by a summer grant from Witchita State University.

References

Bradley, A., Switkes, E., & De Valois, K. (1988). Orientation and spatial frequency selectivity of adaptation to color and luminance gratings. *Vision Research*, *28*, 841–856.

Calkins, D. J., Thornton, J. E., & Pugh, E. N. Jr. (1992). Monochromatism determined at a long-wavelength/middle-wavelength cone-antagonistic locus. *Vision Research*, *32*, 2349–2367.

Chan, H., De Valois, K., & Switkes, E. (1986). Binocular spatial interactions of equiluminant and luminance patterns. *Investigative Ophthalmology & Visual Science*, *27*, 75.

Chaparro, A., Stromeyer, C. F. III, Chen, G., & Kronauer, R. E. (1995). Human cones appear to adapt at low light levels: measurements on the red–green detection mechanism. *Vision Research*, *35*, 3103–3118.

Chaparro, A., Stromeyer, C. F. III, Huang, E. P., Kronauer, R. E., & Eskew, R. T. Jr. (1993). Colour is what the eye sees best. *Nature*, *361*, 348–350.

Chaparro, A., Stromeyer, C. F. III, Kronauer, R. E., & Eskew, R. T. Jr. (1994). Separable red–green and luminance detectors for small flashes. *Vision Research*, *34*, 751–762.

Cicerone, C. M., & Nerger, J. L. (1989). The relative numbers of long-wavelength-sensitive to middle-wavelength-sensitive cones in the human fovea centralis. *Vision Research*, *29*, 115–128.

Cole, G. R., Hine, T., & McIlhagga, W. (1993). Detection mechanisms in L-, M-, and S-cone contrast space. *Journal of the Optical Society of America A*, *10*, 38–51.

Cole, G. R., Hine, T. J., & McIlhagga, W. (1994). Estimation of linear detection mechanisms for stimuli of medium spatial frequency. *Vision Research*, *34*, 1267–1278.

Cole, G. R., Stromeyer, C. F. III, & Kronauer, R. E. (1990). Visual interactions with luminance and chromatic stimuli. *Journal of the Optical Society of America A*, *7*, 128–140.

Derrington, A. M., Krauskopf, J., & Lennie, P. (1984). Chromatic mechanisms in lateral geniculate nucleus of macaque. *Journal of Physiology*, *357*, 241–265.

De Valois, R. L., & Walraven, J. (1967)). Monocular and binocular aftereffects of chromatic adaptation. *Science*, *155*, 463–465.

Eskew, R. T. Jr., McLellan, J. S., & Giulianini, F. (1999). Chromatic detection and discrimination. In K. R. Gegenfurtner, & L. T. Sharpe, *Colour vision: from molecular genetics to perception*. Cambridge: Cambridge University Press (in press).

Finkelstein, M. A., & Hood, D. C. (1984)). Detection and discrimination of small, brief lights: variable tuning of opponent channels. *Vision Research*, *24*, 175–181.

Gegenfurtner, K. R., & Hawken, M. J. (1995). Temporal and chromatic properties of motion mechanisms. *Vision Research*, *35*, 1547–1563.

Giulianini, F., & Eskew, R. T. Jr. (1998). Chromatic masking in the (ΔL/L, ΔM/M) plane of cone-contrast space reveals only two detection mechanisms. *Vision Research*, *38*, 3913–3926.

Gowdy, P. D., & Cicerone, C. M. (1998). The spatial arrangement of the L and M cones in the central fovea of the living human eye. *Vision Research*, *38*, 2575–2589.

Gowdy, P.D., Stromeyer, C.F. III, & Kronauer, R.E. (1999). Facilitation between the luminance and red–green detection mechanisms: enhancing color differences across edges, *Vision Research*, *39* (in press).

Hayhoe, M. M. (1979). After-effects of small adapting fields. *Journal Physiology*, *296*, 141–158.

Knoblauch, K., & Maloney, L. T. (1996). Testing the indeterminacy of linear color mechanisms from color discrimination data. *Vision Research*, *36*, 295–306.

Kleinschmidt, J., & Dowling, J. E. (1975). Intracellular recordings from gecko photoreceptors during light and dark adaptation. *Journal of General Physiology*, *66*, 617–648.

Krauskopf, J., Williams, D. R., & Heeley, D. W. (1982). Cardinal directions of color space. *Vision Research*, *22*, 1123–1131.

Lee, B. B., Martin, P. R., & Valberg, A. (1989). Sensitivity of macaque retinal ganglion cells to chromatic and luminance flicker. *Journal of Physiology*, *414*, 223–243.

Metha, A. B., & Mullen, K. T. (1998). Failure of direction discrimination at detection threshold for both fast and slow chromatic motion. *Journal of the Optical Society of America A*, *15*, 2945–2950.

Mollon, J. D., & Polden, P. G. (1977)). An anomaly in the response of the eye to short wavelengths. *Philosophical Transactions of the Royal Society B*, *278*, 207–240.

Mullen, K. T. (1985). The contrast sensitivity of human colour vision to red–green and blue–yellow chromatic gratings. *Journal of Physiology*, *359*, 381–400.

Mullen, K. T., Cropper, S. J., & Losada, M. A. (1997). Absence of linear subthreshold summation between red–green and luminance mechanisms over a wide range of spatial-temporal conditions. *Vision Research*, *37*, 1157–1165.

Nagy, A. L., Eskew, R. T. Jr., & Boynton, R. M. (1987). Analysis of color-matching ellipses in a cone-excitation space. *Journal of the Optical Society of America A*, *4*, 756–768.

Normann, R. A., & Perlman, I. (1979). The effects of background illumination on the photoresponses of red and green cones. *Journal of Physiology*, *286*, 491–507.

Poirson, A. B., Wandell, B. A., Varner, D., & Brainard, D. H. (1990). Surface characterizations of color thresholds. *Journal of the Optical Society of America A*, *7*, 783–789.

Powell, I. (1981). Lens for correcting chromatic aberration of the eye. *Applied Optics*, *20*, 4152–4155.

Regan, B. C., Reffin, J. P., & Mollon, J. D. (1994)). Luminance noise and the rapid determination of discrimination ellipses in colour deficiency. *Vision Research*, *34*, 1279–1299.

Regan, D., & Tyler, C. W. (1971). Some dynamic features of colour vision. *Vision Research*, *11*, 1307–1324.

Sankeralli, M. J., & Mullen, K. T. (1997). Postreceptoral chromatic detection mechanisms revealed by noise masking in three-dimensional cone contrast space. *Journal of the Optical Society of America A*, *14*, 2633–2646.

Smith, V. C., & Pokorny, J. (1975)). Spectral sensitivity of the foveal cone photopigments between 400 and 500 nm. *Vision Research*, *15*, 161–171.

Sternheim, C. E., Stromeyer, C. F. III, & Khoo, M. C. K. (1979). Visibility of chromatic flicker upon spectrally mixed adapting fields. *Vision Research*, *19*, 175–183.

Stromeyer, C. F. III, Chaparro, A., Tolias, A. S., & Kronauer, R. E. (1997). Colour adaptation modifies the long-wave *versus* middle-wave weights and temporal phases in human luminance (but not red–green) mechanism. *Journal of Physiology*, *499*, 227–254.

Stromeyer, C. F. III, Cole, G. R., & Kronauer, R. E. (1985). Second-site adaptation in the red–green chromatic pathways. *Vision Research*, *25*, 219–237.

Stromeyer, C. F. III, Kronauer, R. E., Ryu, A., Chaparro, A., & Eskew, R. T. Jr. (1995). Contribution of the long-wave and middle-wave cones to motion detection. *Journal of Physiology*, *485*, 221–243.

Stromeyer, C. F. III, Lee, J., & Eskew, R. T. Jr. (1992). Peripheral chromatic sensitivity for flashes: a post-receptoral red–green asymmetry. *Vision Research*, *32*, 1865–1873.

Stromeyer, C. F. III, & Sternheim, C. E. (1981). Visibility of red and green spatial patterns upon spectrally mixed adapting fields. *Vision Research*, *21*, 397–407.

Thornton, J. E., & Pugh, E. N. Jr. (1983). Red/green opponency at detection threshold. *Science*, *219*, 191–193.

Wandell, B. A., & Pugh, E. N. Jr. (1980a). A field-additive pathway detects brief-duration, long-wavelength incremental flashes. *Vision Research*, *20*, 613–624.

Wandell, B. A., & Pugh, E. N. Jr. (1980bb)). Detection of long-duration, long-wavelength incremental flashes by a chromatically coded pathway. *Vision Research*, *20*, 625–636.

Wandell, B. A., Sanchez, J., & Quinn, B. (1982)). Detection/discrimination in the long-wavelength pathways. *Vision Research*, *22*, 1061–1069.

Watson, A. B., & Robson, J. G. (1981). Discrimination at threshold: labelled detectors in human vision. *Vision Research*, *21*, 1115–1122.

Watson, A. B., & Turano, K. (1995). The optimal motion stimulus. *Vision Research*, *35*, 325–336.

Webster, M. A., De Valois, K. K., & Switkes, E. (1990). Orientation and spatial-frequency discrimination for luminance and chromatic gratings. *Journal of the Optical Society of America A*, *7*, 1034–1049.

Wetherill, G. B. (1963). Sequential estimation of quantal response curves. *Journal of the Royal Statistical Society B*, *25*, 1–48.

Yang, J., Qi, X., & Makous, W. (1995)). Zero frequency masking and a model of contrast sensitivity. *Vision Research*, *35*, 1965–1978.

Yeh, T., Lee, B. B., & Kremers, J. (1996). The time course of adaptation in macaque retinal ganglion cells. *Vision Research*, *36*, 913–931.